Supporting information

Photochemistry of Thin Solid Films of the Neonicotinoid Imidacloprid on Surfaces

Kifle Z. Aregahegn,[1] Dorit Shemesh,[2] R. Benny Gerber[1,2] and Barbara J. Finlayson-Pitts[1]

[1]Department of Chemistry, University of California, Irvine, CA 92697
[2]Department of Physical Chemistry and the Fritz Haber Research Center, The Hebrew University, Jerusalem 91904, Israel

Number of Pages: 18

Number of figures: 10

Number of tables: 8

1. PHOTOLYSIS MECHANISM

A typical IMD photolysis mechanism proposed by Shipper and Schwack[1] in solution is given in Scheme S-1. The photolysis process proceeds either by formation of the nitroso derivative or by the release of $-NO_2$. A similar mechanism has been reported for IMD photolysis on tomato leaves[2] and glass surfaces.[1]

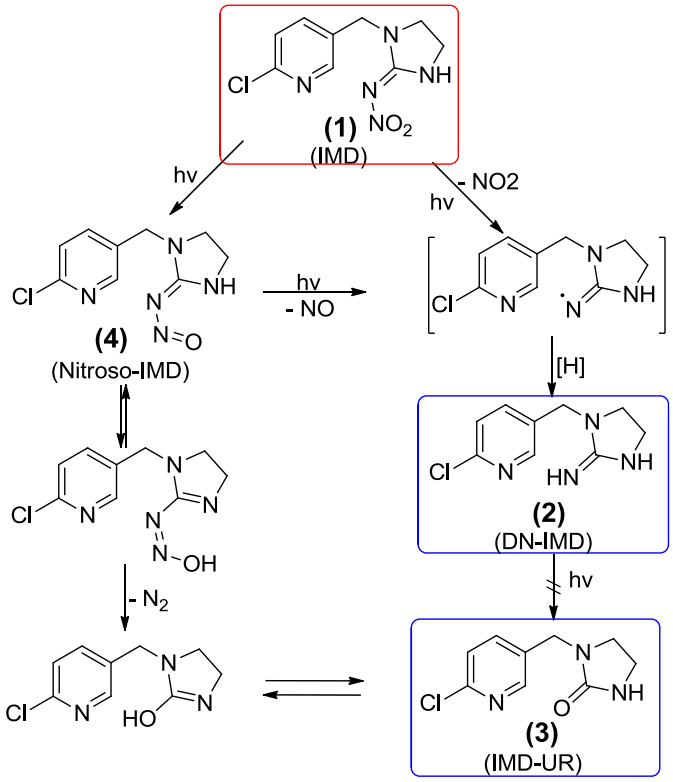

Scheme S-1. Proposed photolysis mechanism of imidacloprid in aqueous solutions and on tomato leaves.[1, 2]

2. MATERIALS AND METHODS

Imidacloprid (IMD) and desnitro-imidacloprid (DN-IMD) standards were used as received (Fluka, Germany, both 99.9%,) and imidacloprid urea (IMD-UR) (Chemservice Inc, USA, 98.6%) were used as received. Solutions of IMD for coating the ATR-crystal were prepared by dissolving the standard sample in acetonitrile (ACS Grade, 99.5%). The ATR-crystal was cleaned first by boiling in dichloromethane (ACS Grade) and rinsing with nanopure water (18.2 MΩ-cm). The IMD solution was atomized onto the desired area of the ATR crystal using a commercial atomizer (TSI Model 3076) and a custom made Teflon holder

that had the same opening size as the ATR reaction cell (Figure S-1). The sample was dried in air before ATR-FTIR analysis.

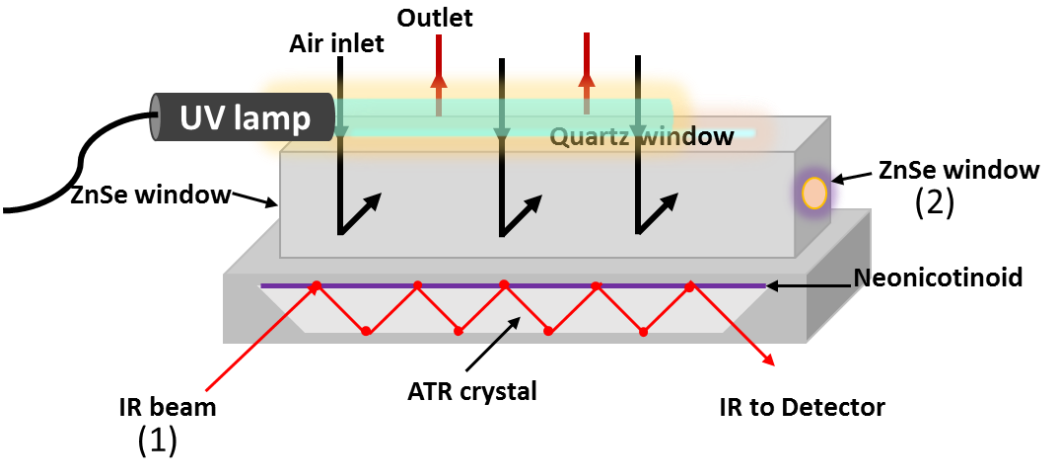

Figure S-1: Schematic of the ATR reaction cell.[3]

3. UV/VIS ABSORPTION SPECTRA OF IMD AND ITS DERIVATIVES

UV/Vis absorption spectra (200-350 nm) of the standard compounds, IMD, IMD-UR and DN-IMD, were measured using a diode array spectrophotometer (HP 8452A) (Fig. S-2). The solutions were prepared by dissolving the reagents in acetonitrile and average absorption cross-sections were calculated from the absorbance as a function of concentration using a quartz cuvette (Crystal Laboratories, path length = 1 mm). Table S-1 summarizes the molar absorption coefficients from this study as well as some reported in the literature.

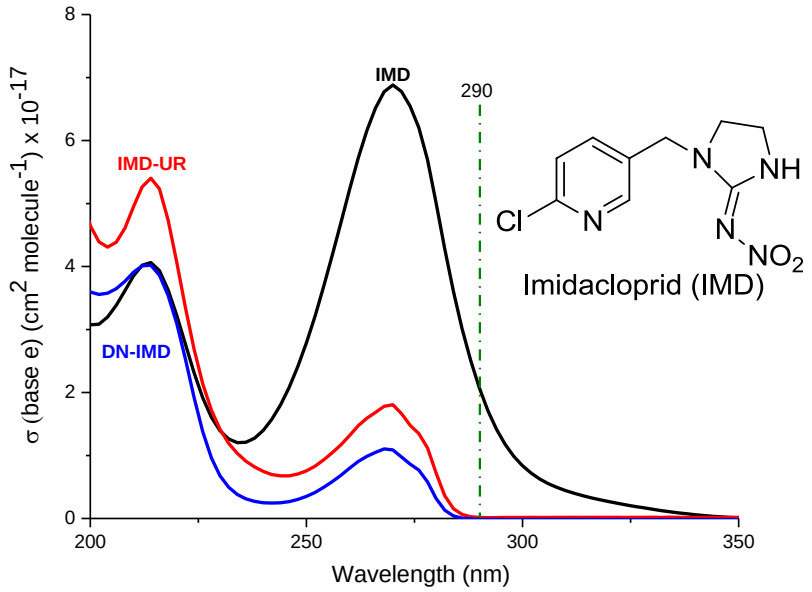

Figure S-2: UV absorption cross sections of imidacloprid (IMD, 0.6 mM in methanol (99.9%, OmniSolv), imidacloprid urea (IMD-UR, 0.5 mM in methanol (99.9%, OmniSolv) and desnitro-imidacloprid (DN-IMD, 0.5 mM in nanopure water (18 MΩ-cm)) in 1 mm path length quartz cell.

Table S-1: Molar absorption coefficients (ε, M^{-1} cm^{-1}, base 10) of IMD at 254 nm, 270 and 305 nm.

ε_{254nm}	ε_{270nm}	ε_{305nm}	Reference
1.12×10^4	2.19×10^4	2.64×10^3	This work
1.09×10^4			Dell'Arciprete *et al.*[4]
~1.55×10^4 [a]	~1.86×10^4 [a]	~ 3.10×10^3 [a]	Lu *et al.*[5]

[a]Estimated from absorption spectra.

4. PHOTOLYSIS LAMP CHARACTERISTICS AND QUANTUM YIELD DETERMINATION

The emission spectra for the two lamps used in this study were measured using an Ocean Optics spectrometer (model HR 4000 CG-UV-NIR) are shown in Figure S-3.

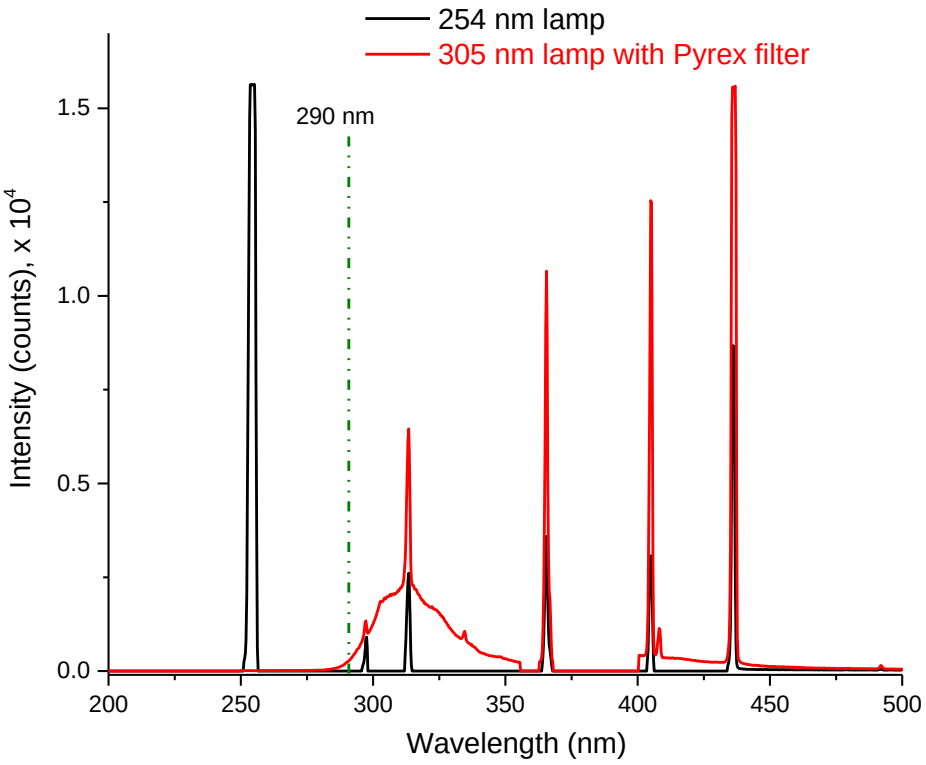

Figure S-3: Relative emission spectra of UV lamps.

The low pressure mercury lamp has a strong line at 254 nm, and weaker line at 297 and 313 nm that are within the absorption window for IMD (Fig. S-2). The 305 nm lamp has a broadband emission out to ~ 360 nm due to the organic phosphor coating, along with superimposed mercury lines. A pyrex glass cover slide was placed in front of the 305 nm lamp to restrict the UV to wavelengths below 290 nm.

Absolute light intensities for the two lamps which are needed to determine quantum yields for loss of imidacloprid were measured using 2-nitrobenzaldehyde (2-NB) as an actinometer. 2-nitrobenzaldehyde converts photochemically into 2-nitrosobenzoic acid:

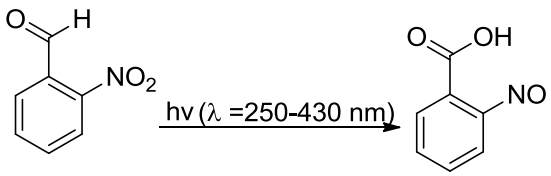

2-nitrosobenzoic acid

To measure absolute light intensities,[6-10] a known mixture of 2-NB and potassium bromide (KBr) was used, where sufficient 2-NB was present to absorb all of the photons. The quantum yield (ϕ) of 2-NB from 250-430 nm has been reported to be 0.5 as a solid or in solution,[6-10] although Anastasio and coworkers[10] recently reported a value of 0.41 for solutions. We assume ϕ = 0.5 since this is what has been reported for 2-NB in pressed KBr pellets similar to what was used here.[7] Samples were prepared by mixing various amounts of 2-NB (Fluka, ≥ 99.0 %) with 1.19 g of KBr (Fisher, ACS Grade). The mixtures were well ground and pressed under vacuum into pellets of 1.29 cm diameter and 0.04 cm average thickness under a pressure of 5000 psi. The pellet was then placed in the same configuration as the sample during photolysis in such a way that the IR beam passed through the pellet which was irradiated at 305 nm or 254 nm. The decrease in the 2-NB peak at 1350 cm^{-1} was followed with time in the transmission mode. Figure S-4a shows the spectrum of 2-NB before photolysis and the difference spectrum after photolysis at 254 nm.

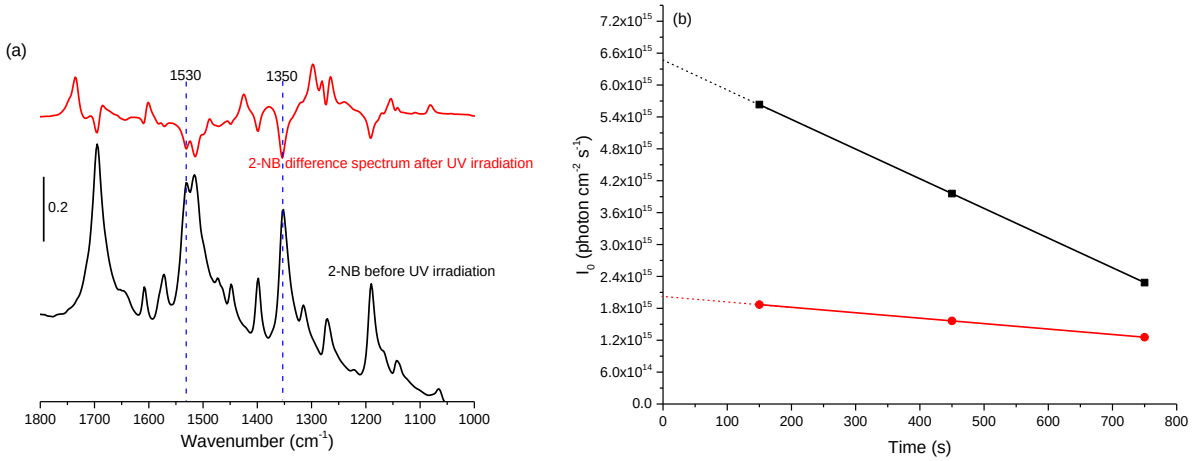

Figure S-4: Absolute light intensity determination using 2-NB as an actinometer; (a) FTIR spectrum of 2-NB in KBr before photolysis and the difference spectrum after irradiation at 254 nm. The difference spectrum is log (S_0/S_1) where S_0 is the single beam spectrum before photolysis and S_1 is that after photolysis. Negative peaks represent loss of 2-NB while positive peaks represent new products formed. (b) relationship between absorbed light intensities and time of exposure for one measurement at 254 nm (black squares) and one for the 305 nm lamp (red circles).

The relative intensity of the photolysis lamps, $I_{rel}(\lambda)$ is related to the absolute light intensity, $I_{abs}(\lambda)$, through a correction factor, *CF*:

$$I_{abs}(\lambda) = CF * I_{rel}(\lambda) \quad (1)$$

The correction factor (CF) for each lamp was obtained as follows: (1) the number of 2-NB molecules in the pellet is determined from the relative weights of 2-NB and KBr used to make the mixture, and the total mass of the pellet; (2) the loss of 2-NB molecules with time (Δ2-NB/Δt) is determined as a function of irradiation time (t) from the change in absorbance at 1350 cm^{-1} due to 2-NB, (ΔA/Δt). This is equivalent to half the number of photons absorbed per unit time, based on a quantum yield of 0.5; (3) the value of (Δ2-NB/Δt) decreases with time due to shielding by the products,[7] so that this rate was extrapolated back to t = 0 (Fig. S-4b) to obtain the initial total photon flux, I_0 (photons cm^{-2} s^{-1}). The value of I_0 was measured to be 6.5×10^{15} photons cm^{-2} s^{-1} for the 254 nm lamp and 1.9×10^{15} photons cm^{-2} s^{-1} for the 305 nm broadband lamp.

With the correction factor thus determined, the quantum yield for IMD was calculated from the measured photolysis rate constants (k_p) for IMD using:

$$k_p = \phi \sum_{\lambda} I_{rel}(\lambda)\sigma(\lambda) * CF \quad (2)$$

where σ(λ) is the absorption cross section of IMD as a function of wavelength (Fig. S-2) and ϕ is the photolysis quantum yield assumed to be independent over the emission region of the lamp.

Figure S-5 shows typical decays for IMD during photolysis at 254 nm (Fig S-5a) or using the 305 nm broadband (Fig. S-5b) lamps.

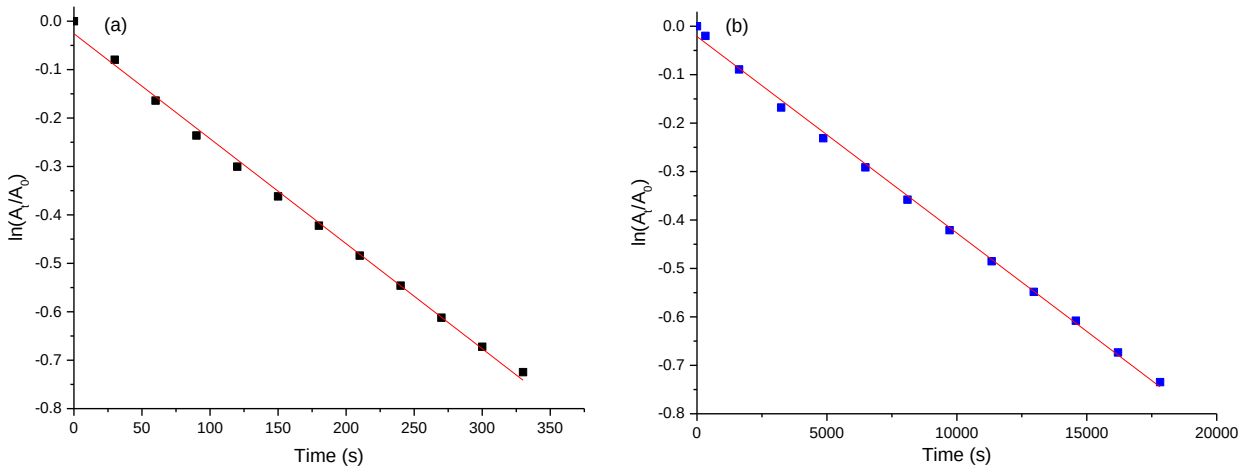

Figure S-5: Typical first order decays of imidacloprid from which photolysis rate constants were obtained; (a) 254 nm and (b) 305 nm. Values for individual runs and average values at each wavelength are given in Table S-2.

The different experiment done to determine k_p and ϕ of IMD for 305 nm and 254 nm irradiation are summarized in Table S-2.

Table S-2: Estimated photolysis rate constants[a] and quantum yields for imidacloprid on a Ge ATR crystal at different irradiation wavelengths

Experiment	lamp	$k_p(s^{-1})$	ϕ
1	305 nm	1.1×10^{-5}	1.2×10^{-3}
2	305 nm	1.1×10^{-5}	1.2×10^{-3}
3	305 nm	2.5×10^{-5}	2.6×10^{-3}
4	305 nm	2.0×10^{-5}	2.1×10^{-3}
5	305 nm	1.7×10^{-5}	1.8×10^{-3}
6	305 nm	1.2×10^{-5}	1.2×10^{-3}
7	305 nm	1.1×10^{-5}	1.2×10^{-3}
Average (305 nm)		**$(1.5 \pm 0.5) \times 10^{-5}$ [b]**	**$(1.6 \pm 0.6) \times 10^{-3}$ [b]**
1	254 nm	1.1×10^{-3}	0.6×10^{-2}
2	254 nm	1.2×10^{-3}	0.6×10^{-2}
3	254 nm	1.9×10^{-3}	1.0×10^{-2}
4	254 nm	2.0×10^{-3}	1.1×10^{-2}
5	254 nm	2.1×10^{-3}	1.1×10^{-2}
6	254 nm	1.4×10^{-3}	0.7×10^{-2}
7	254 nm	1.7×10^{-3}	0.9×10^{-2}
8	254 nm	1.4×10^{-3}	0.8×10^{-2}
Average (254 nm)		**$(1.6 \pm 0.4) \times 10^{-3}$ [b]**	**$(8.5 \pm 2.1) \times 10^{-3}$ [b]**

[a]Determined by following IMD out to 30-50% loss. [b]Errors are ± 1s.

5. DART-MS CONFIGURATION

Figure S-6 shows the DART-MS and sample screen configuration.

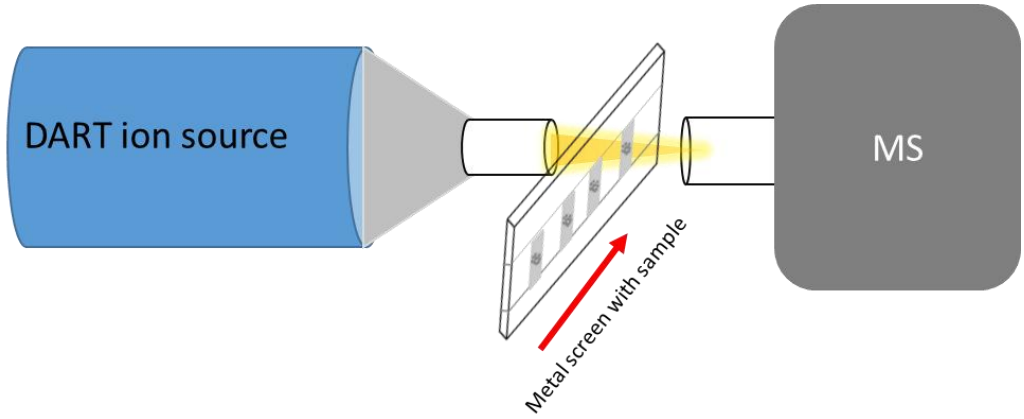

Figure S-6: Schematic for DART-MS analysis of imidacloprid.

6. THEORETICAL CALCULATIONS

Vertical excitation energies for the lowest energy conformer (see Figure 3 in text), namely IMI-1a from ref. (48) were calculated using a high-level *ab initio* method, ADC(2) for both chlorine-containing IMD as well as the analogous fluorine compound. The results gave similar transitions (Tables S-2, 3) It is therefore justified to use the fluorine analogue for the semi-empirical OM2/MRCI calculations, since parameters for chlorine are not available for this method. Results are shown in Table S-4. The semiempirical method predicts the strongest transition is the first one, whereas the ADC(2) method predicts the first strong transition as state 3. Those states are the same excitation, as confirmed by the same orbital transitions involved. We assume that the experimental transition is to the this state. The molecular dynamics simulation using the semiempirical method starts therefore on the first excited state.

Table S-3: Transitions predicted for IMD-1a with chlorine using ADC(2)/cc-pVDZ

State	Vertical excitation energy (in eV)	Oscillator strength
1	3.94	0.00006
2	4.93	0.0006
3	5.07	0.13
4	5.14	0.26
5	5.29	0.007

Table S-4: Transitions predicted for IMD-1a with fluorine using ADC(2)/cc-pVDZ

State	Vertical excitation energy (in eV)	Oscillator strength
1	3.93	0.000095
2	4.93	0.0005
3	5.10	0.26
4	5.18	0.14
5	5.46	0.004

Table S-5: Transitions predicted for the fluorine analog of imidacloprid IMD 1a using the semi-empirical OM2/MRCI method

State	Vertical excitation energy (in eV)	Oscillator strength
1	4.95	0.57
2	5.45	0.29
3	5.48	0.0006
4	5.73	0.031

7. CALCULATIONS OF TYPICAL PHOTOLYSIS RATE CONSTANT IN TROPOSPHERE

The photolysis rate constant (k_p) for noon at a latitude of 40°N on April 1 was calculated from:

$$k_p = \sum_{\lambda} \mathrm{F}(\lambda)\sigma(\lambda)\phi\mathrm{D} \qquad (3)$$

where F(λ) is the actinic flux, σ(λ) are the absorption cross sections determined here, $\phi = 1.6 \times 10^{-3}$ is the quantum yield for IMD at 305 nm measured here and assumed to be wavelength independent, and D is the earth-sun distance correction factor.[11]

8. RESULTS: PHOTOLYSIS PRODUCT YIELDS

8A. DART-MS AND ESI-MS DATA

The molar ratio of the two products formed on the surface was measured using ESI-MS and DART-MS. Figure S-7a shows the ratio of the peak intensities for the DN-IMD to IMD-UR product as a function of the molar ratio of concentrations in calibration mixtures. IMD-UR had an $[M+Na]^+$ peak in ESI-MS and hence the total peak intensity is the sum of the $[M+H]^+$ and $[M+Na]^+$ peaks (the relative intensities of $[M+H]^+$ and $[M+Na]^+$ are similar). However, DN-IMD does not form a sodium adduct so the$[M+H]^+$ peak alone was used.

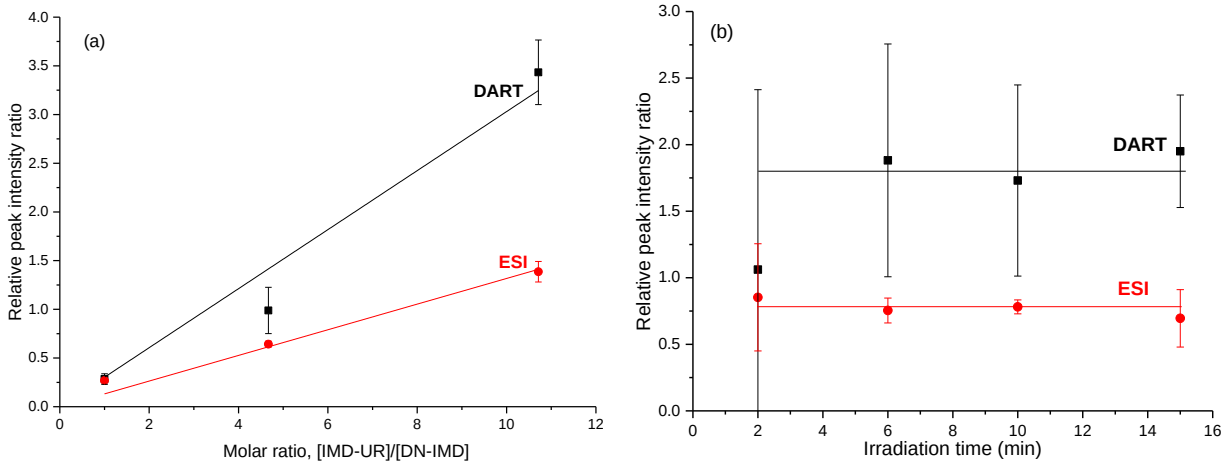

Figure S-7: (a) The ratio of relative peak intensities for the products IMD-UR (*m/z* 212 + m/z 234*) to DN-IMD (*m/z* 211) in calibration mixtures as a function of the molar ratio in standard solutions using ESI-MS (red circles) or DART-MS (black squares); (b) the ratio of peak intensities due to IMD-UR (*m/z* 212 + m/z 234*) and DN-IMD (*m/z* 211) using DART-MS (black squares) and ESI-MS (red circles) for increasing IMD photolysis times. * Sodiated peak for IMD-UR appears only in ESI-MS analysis.

Table S-6: Relative rates of production of the photolysis products desnitro-imidacloprid and imidacloprid-urea at different irradiation wavelengths and irradiation times

Experiment #	Technique	Lamp (nm)	Irradiation time	Molar ratio [IMD-UR]/[DN-IMD][a,b]
1	ESI	305	1 h	4.0 ± 0.1
2		305	2 h	4.4 ± 0.4
3		305	3 h	4.3 ± 0.02
4		305	4h	4.4 ± 0.7
Average (ESI, 305 nm)				**4.3 ± 0.2**
1	DART	305	1 h	5.6 ± 0.7
2		305	2 h	5.2 ± 1.4
3		305	3 h	4.7 ± 1.2
4		305	4 h	5.1 ± 0.5
Average (DART, 305 nm)				**5.2 ± 0.4**
1	ESI	254	6 min	6.5± 3.1
2		254	10 min	5.7± 0.7
3		254	15 min	5.9± 0.4
Average (ESI, 254 nm)				**6.0 ± 0.4**
1	DART	254	6 min	6.2 ± 2.9
2		254	10 min	5.7 ± 2.4
3		254	15 min	6.4 ± 1.4
Average (DART, 254 nm)				**6.1 ± 0.1**

[a]Error bars are ± 1s.
[b]Average of two runs.

8B. N_2O DATA

The reaction cell was calibrated for N_2O by making mixtures of measured pressures of N_2O with air (Praxair, Ultra zero) on a vacuum rack, introducing the mixtures into the ATR cell, and carrying out transmission FTIR. In some experiments, N_2O formation was followed with photolysis time (Fig. S-8) but in that case, the solid could not be followed simultaneously. In order to obtain yields of N_2O, the loss of IMD was followed with time and N_2O measured at the end of the experiment. The yields of N_2O yield are summarized in Table S-8.

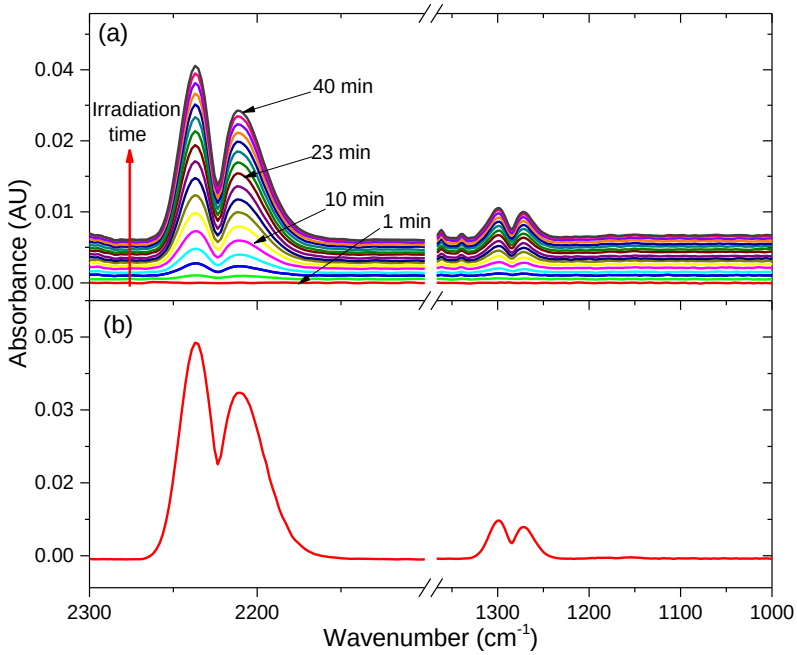

Figure S-8: (a) FTIR transmission spectra of gaseous N_2O formed during IMD 254 nm irradiation; (b) 417 ppm N_2O calibration standard in air.

Table S-7: Nitrous oxide yields from imidacloprid direct photolysis on a Ge ATR crystal at 305 and 254 nm

Experiment #	Lamp (nm)	$\Delta[N_2O]/\Delta[IMD]$
1	305	0.96
2	305	0.62
3	305	0.52
4	305	0.95
5	305	0.77
6	305	1.06
7	305	1.27
Average		**0.88 ± 0.26**[a]
1	254	0.75
1	254	0.49
2	254	0.53
3	254	0.50
4	254	0.52
5	254	0.44
6	254	0.46
Average		**0.53 ± 0.10**[a]

[a]Error bars are ± 1s.

9. RESULTS: THEORETICAL CALCULATION INSIGHT

Table S-8: Statistics of the photochemistry at 254 nm

Pathway	Number of trajectories
NO_2 cleavage	85
H transfer and OH abstraction	2
Aborted trajectories	9
H transfer, HONO formation	1
Different pathways	3

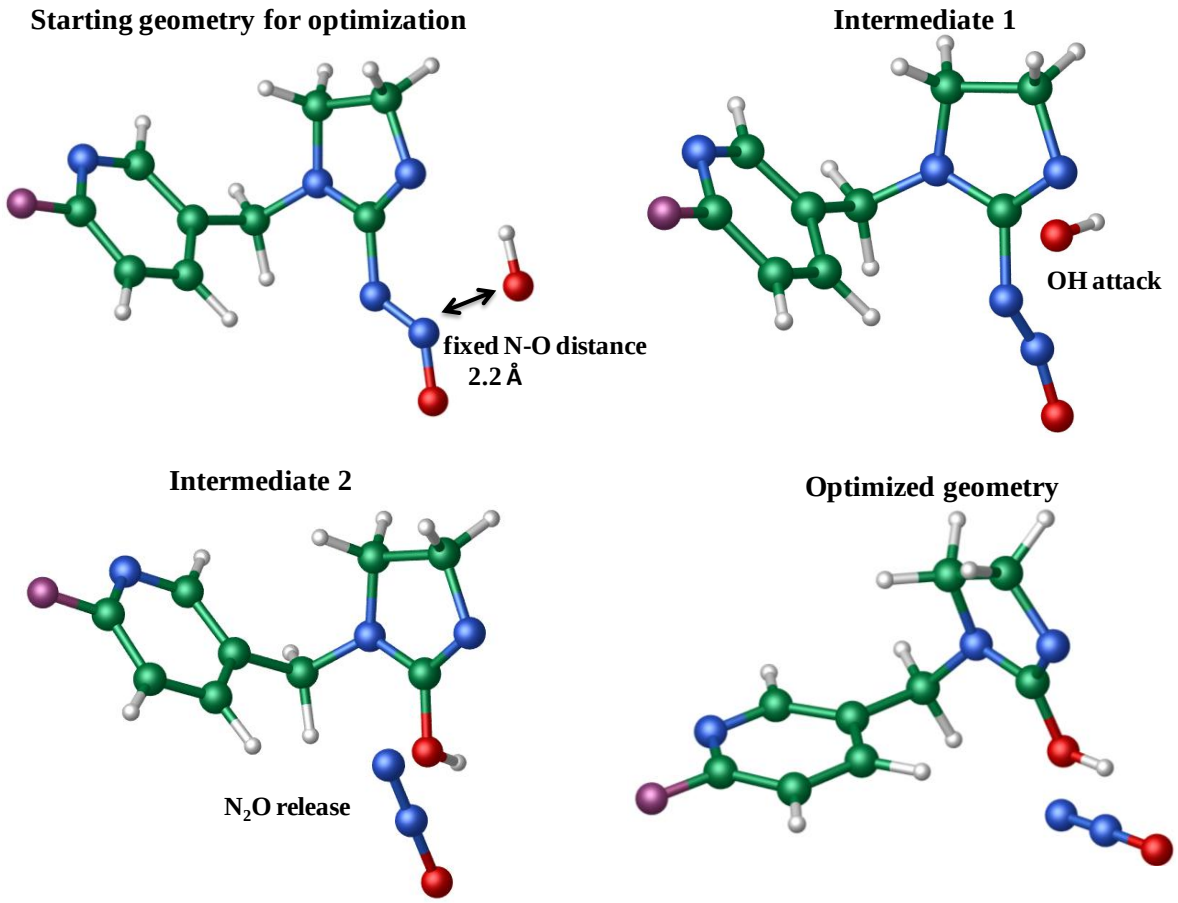

Figure S-9: Snapshots of the optimization at the N-O distance of 2.2 Å.

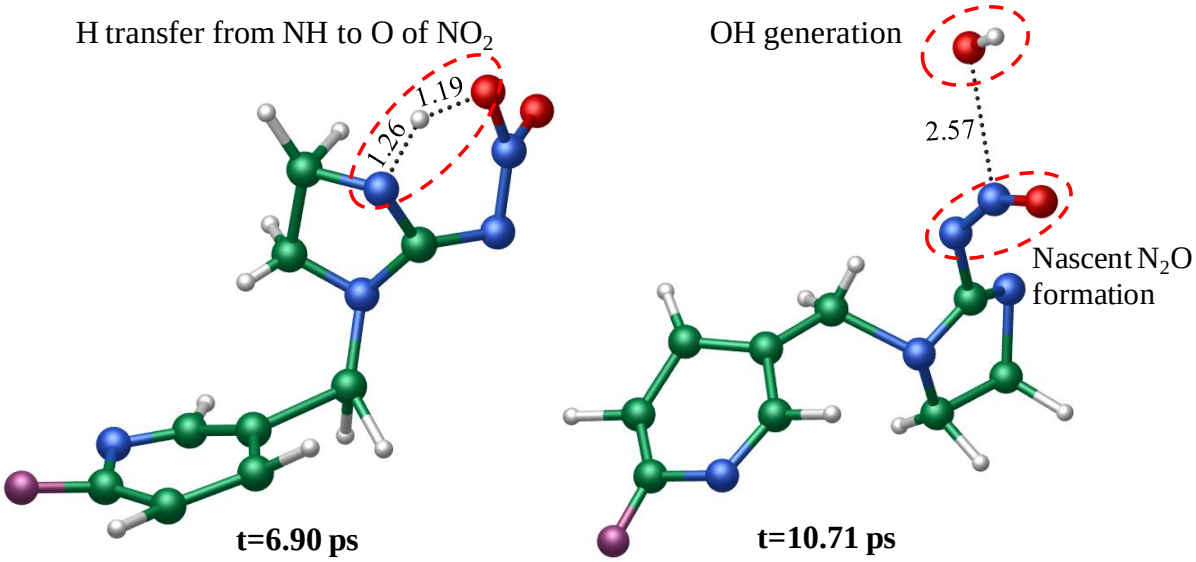

Figure S-10: Snapshots of the minor mechanism for N_2O formation occurring on the excited state.

REFERENCES

1. Schippers, N.; Schwack, W., Photochemistry of imidacloprid in model systems. *J. Agri. Food Chem.* **2008,** *56*, (17), 8023-8029.
2. Scholz, K.; Reinhard, F., Photolysis of imidacloprid (NTN 33893) on the leaf surface of tomato plants. *Pest. Sci.* **1999,** *55*, (6), 652-654.
3. Moussa, S. G.; Finlayson-Pitts, B. J., Reaction of gas phase OH with unsaturated self-assembled monolayers and relevance to atmospheric organic oxidations. *Physical Chemistry Chemical Physics* **2010,** *12*, (32), 9419-9428.
4. Dell'Arciprete, M. L.; Santos-Juanes, L.; Sanz, A. A.; Vicente, R.; Amat, A. M.; Furlong, J. P.; Martire, D. O.; Gonzalez, M. C., Reactivity of hydroxyl radicals with neonicotinoid insecticides: mechanism and changes in toxicity. *Photochem. Photobiol. Sci.* **2009,** *8*, (7), 1016-1023.
5. Lu, Z.; Challis, J. K.; Wong, C. S., Quantum yields for direct photolysis of neonicotinoid insecticides in water: implications for exposure to nontarget aquatic organisms. *Environ. Sci. Technol. Lett.* **2015,** *2*, (7), 188-192.
6. Leighton, P. A.; Lucy, F. A., The photoisomerization of the o-nitrobenzaldehydes I. photochemical results. *J. Chem. Phys.* **1934,** *2*, (11), 756-759.
7. Pitts, J. N.; Wan, J. K. S.; Schuck, E. A., Photochemical studies in an alkali halide matrix. I. An o-nitrobenzaldehyde actinometer and its application to a kinetic Study of the photoreduction of benzophenone by benzhydrol in a pressed potassium bromide disk. *J. Amer. Chem. Soc.* **1964,** *86*, (18), 3606-3610.
8. Vichutinskaya, Y. V.; Postnikov, L. M.; Kushnerev, M. Y., The use of o-nitrobenzaldehyde as internal actinometer when studying photo-oxidative breakdown of thin unoriented polycaprolactam films. *Polymer Sci. U.S.S.R.* **1975,** *17*, (3), 716-721.
9. Allen, J. M.; Allen, S. K.; Baertschi, S. W., 2-Nitrobenzaldehyde: a convenient UV-A and UV-B chemical actinometer for drug photostability testing. *J. Pharm. Biomed. Anal.* **2000,** *24*, (2), 167-178.
10. Galbavy, E. S.; Ram, K.; Anastasio, C., 2-Nitrobenzaldehyde as a chemical actinometer for solution and ice photochemistry. *J. Photochem. Photobiol A-Chemistry* **2010,** *209*, (2-3), 186-192.
11. Finlayson-Pitts, B. J.; Pitts, J. N., *Chemistry of the upper and lower atmosphere : theory, experiments, and applications*. Academic Press: San Diego, **2000**; p xxii, 969 p.